OPTIMIZATION STUDY FOR AN INTERNAL SUPPORTING FLANGE IN A NUCLEAR REACTOR VESSEL

S. CURIONI, P. NERI,

Comitato Nazionale per l'Energia Nucleare, Programma Reattori Veloci, Bologna, Italy

ABSTRACT

An optimization study for the supporting flange of the core element grid in a nuclear fast reactor is done in the first part of this work; we are investigate on the influence that the most interesting geometrical parameters have on the range of the structure stresses.

Some consideration on the limits of applicability of the simplified theory of the axialsymmetrical rings are done in the second part, by comparing the results obtained with the different structures examined.

1) Introduction

The vessel used in the sodium-cooled fast reactors must meet particular requirements which significantly differentiate them from the same components used in the chemical plants and in other nuclear units.

In addition to the choice of a material compatible with the coolant used, these requirements impose also a detailed structural analysis for the presence of remarkable local loads applied to the vessel and of axial pressure gradients. Infact the support grid of the fuel elements divides two zones with different pressure, like in the other nuclear systems, and this pressure drop is tied to the loss of pressure in the core elements; in the sodium fast reactors this pressure drop is very high as compared with that of the most conventional reactors owing to the high thermal flux generated in the core involving the need to make sodium circulate at a high speed in order to remove all the heat produced. In addition it is not necessary to pressurize those fluids to rise the boiling temperature since this has already a satisfactory value at atmospheric pressure. As a consequence of what above said the loca-

lized loads applied to the vessel by the grid resulting not only from the fuel elements weight but also from the pressure exerted from these grids by the inlet coolant and the axial pressure gradient, are the most important loads to which the structure is submitted.

The first present work objective is to optimize this zone of the vessel by investigating on the influence that the most interesting geometrical parameters have on the range of the structure stresses and deformation; the necessity of optimization is due other than to the particular load conditions to which those components are subjected as already seen, also to the considerable cost that they present (Fig. 1).

The second present work objective is to investigate on the limits of applicability of the simplified theory of the axialsymmetrical rings utilized in the first part, by comparing the results obtained in some cases where different methods of resolution could be applied. To this end a structure has been examined formed by two cylindrical shells of different thickness, radiused by a cylindrical shell with a wall of a linearly variable thickness; for the comparison a structure has been considered with the same conditions of constraint and load, where the two cylindrical shells are connected by a cylindrical shell of a mean thickness as compared by the other two (Fig. 2).

2) Methodology used

The solution of the problem is obtained by using the Reissner theory |1| and by applying this theory to the conic shell, to the cylindrical shell with a wall of costant thickness and to the cylindrical shell with a wall of a linearly variable thickness (Fig. 1).

a) Cylindrical shell with a wall of constant thickness.
In the case of a cylindrical shell with a wall of constant thickness, the solving equations, are represented by (see Zudans et al. |2|):

$$(E\chi)'' + \frac{1}{d^{*}} H = 0$$
$$(H)'' - \frac{h}{a^2} (E\chi) = \nu\gamma \frac{h}{a} \qquad (1)$$

b) Cylindrical shell with a wall of a linearly variable thickness.
In the case of cylindrical shell with a wall of a linearly variable thickness the solving equations are represented by (see Zudans et al. |2|):

$$(E\chi)'' + \frac{3}{x}(E\chi)' + \frac{1}{ad''}(aH) = 0$$

$$(a\,H)'' - \frac{1}{x}(aH)' - \frac{t}{a}\,x\,(E\chi) = \frac{1}{x}\left[pa - \nu\, N_{i,1}\right] \qquad (2)$$

c) Conic shell

In the case of conic shell with a wall of constant thickness, the solving equations are represented by (see Zudans et al. |2|):

$$(E\chi)'' + \frac{1}{s}(E\chi)' - \frac{1}{s^2}(E\chi) + \frac{c}{d''}\frac{1}{s}(sH) = \frac{b^2}{2d''}\frac{s - s_1^2}{s}\,p + \frac{b}{d''}\frac{1}{s}\,s_1\,N_{i,1} \qquad (3)$$

$$(sH)'' + \frac{1}{s}(sH)' - \frac{1}{s^2}(sH) - \frac{ch}{b^2}\frac{1}{s}(E\chi) = -\frac{c}{2}\left(3 + \frac{s_1^2}{s^2}\right)p + \frac{c}{b}\frac{1}{s^2} + s_1\,N_{i,1}$$

d) Axialsymmetrical ring

For the connecting axialsymmetrical rings submitted to statical loads, the solution pointed out by Biezeno et al. |3| has been adopted. In this case, the solving equations are:

$$E\chi = \frac{K}{Iy}\,\Sigma_t\, a_t\left[-(r_t - r'')\,H_t + M_t + (a_t - K)\,N_t\right]$$

$$Eu_j = \frac{\pi\,(1 - \nu)\,a_j}{V}\,\Sigma_t\, H_t a_t^2 + \frac{1 + \nu}{2\,Pa_j}\,\Sigma_t H_t - E\chi\,(r_j - r'') \qquad (4)$$

3) Definition of the unknown constants

In order to derive the unknown constants, there have been imposed the equilibrium and congruence conditions relative to the links among the bodies and the conditions to the boundary. As a condition to the boun dary it has been imposed that the structure upper end be free and the lower end be fixed.

4) Results

4.1.) In figs. 3,4,5,6,7,8,9 and 10 are given the results obtained in the optimization study for the structure of fig. 1.

4.1.1.) In figs. 3,4,5 and 6 are given, as nondimensional quantities, the maximum values of the axial normal stresses, as function of ε and $\frac{h_3}{h_1}$, for h_1 = 50, 60, 70 and 80 mm. respectively.
From the analysis of the given figures, it can be noted that:

1) for values of the ratio h_3/h_1 included from 0,8 to 1.8, $(\sigma_\phi)_{1,2}$ increases and $(\sigma_\phi)_{3,1}$ reduces as ε increases.

2) For h_3/h_1 = 0.4, $(\sigma_\phi)_{1,2}$ presents a minimum and $(\sigma_\phi)_{3,1}$ a maximum within ε = 32°.

3) The stress $(\sigma_\phi)_{1,2}$ decreases and the stress $(\sigma_\phi)_{3,1}$ increases as the ratio h_3/h_1 increases.

4) The value of ε for which the stresses in the upper section of the cylindrical shell and in the lower section of the conic shell are equal, is as much higher as the h_3/h_1.

From the comparative analysis of the four charts, when h_1 increases it can be noted that:

1) the stresses of the two considered sections reduce and the influence of the ratio h_3/h_1 and of the angle ε on the stresses range attenuate.

2) A flattening of the curves occurs as ε varies. The stresses in the two examined sections are equal, for ratios h_3/h_1 included from 0.6 to 0.4 and for values of the slope which in a first approximation do not change as h_1 changes.

4.1.2.) In figs. 7, 8, 9 and 10 are given, as nondimensional quantities, the maximum values of the circumferential normal stresses depending on ε and h_3/h_1, for h_1 = 50, 60, 70 and 80 mm. respectively. From the analysis of the curves given in fig. 7, it can be noted that:

1) in the upper section of the cylindrical shell the normal circumferential stresses have the same course of the normal axial stresses, except for the behaviour of $(\sigma_\phi)_{1,2}$ for values of h_3/h_1 included between 1,2 and 1,8 and of ε included between 20° and 45°; in this field the sign of $(n_0)_{1,2}$ changes and the point of the section where the stress

reaches its maximum value moves to the opposite side the mean surface of the shell.

2) In the lower section of the conic shell, for ratios of h_3/h_1 included between 1,8 and 1, $(\sigma_\theta)_{3,1}$ decreases as increases and it reaches its minimum for as much high values of ε as the ratio h_3/h_1 is low.
For the above values of the ratio h_3/h_1, it can be noted a sharp increase of $(\sigma_\theta)_{3,1}$ near as much high values of ε as the value of h_3/h_1 is low: in this field the sign of $(m_\theta)_{3,1}$ changes and the point of the section where the stress reaches its maximum value moves to the opposite side of the mean surface of the shell.
For values of h_3/h_1 included between 0,8 and 0,6 $(\sigma_\theta)_{3,1}$ decreases as ε increases.
For $h_3/h_1 = 0,4$, $(\sigma_\theta)_{3,1}$ presents a maximum at about $\varepsilon = 27°$.

3) For values of h_3/h_1 included between 0,4 and 1,2, there exist values of ε for which the circumferential stresses are equal in the two sections examined and they are as much high as the value of the ratio h_3/h_1 is low.

From the comparative analysis of the four charts, as the thickness of the cylindrical shell increases it can be noted that:

1) the stresses in the two sections considered decrease;

2) Here can be still found some values of the angle ε for which the stresses in the two considered sections are equal; but there is both a reduction of the field of values h_3/h_1 and a reduction of the angle ε for which such equality takes place.

In conclusion, from the examination of such figures, it can be derived that the course of the stresses remains similar in the four cases considered.

4.1.3.) Conclusions

For a good utilisation of the material it is convenient that the stress distribution be as much uniform as possibile in all sections of the structure. The objective of this work is just that of assessing such behaviour as some characteristic geometrical parameters vary. In this respect is should be noted that for values of the angle ε included between 20° and 75°, it is

possible to obtain the same value of the axial stresses in the two sections examined with ratios $h_3/h_1 \leq 0,8$; as the ratio h_3/h_1 decreases, the value of these stresses increases (the increase of such value is considerable enough, since when passing from $h_3/h_1 = 0,8$ to $h_3/h_1 = 0,4$ there is an increase of about 40% for $h_1 = 50$ mm.) and the equality takes place for higher and higher values of ε.

Also for the circumferential stresses, there are values of ε included between 30° and 75° for which these stresses have the same value; such equality exists for values of $h_3/h_1 \leq 1$ and even in this case such ratio decreases as the value of these stresses increases and the equality takes place for higher and higher values of ε.

These considerations hold for all the values of h_1 considered.

As for the displacements and rotations, there is an increment in these quantities when increasing the angle ε and reducing the ratio h_3/h_1.

It can be concluded that in order to obtain acceptable values of the stresses without having recourse to materials with remarkable thicknesses, it is suitable to use conic shells with values of the angle of inclination ε included between 20° and 30°; in this field with $h_3/h_1 = 0,8$ it is possible to obtain equal values of the axial stresses in the two sections. In case that these values were not acceptable for the angle ε(i.e.: owing to the presence of thermal and neutronic shields which impose an increment of the section of the vessel above the grid support), it will be suitable to resort to values of $h_3/h_1 < 0,8$ in order to obtain the same values of the axial stresses in the two sections.

4.2.) In the figs. 11, 12, 13, 14, 15, 16, 17, 18 have been given the results obtained in the study about the limits of applicability of the theory of the axialsymmetric rings (see fig. 2).

4.2.1.) In figs. 11, 12, 13 and 14 the course has been plotted of the axial moments and radial displacements in the lower and upper section of the connecting cylinder, in function of l_2, for different values of the ratio h_1/a and for $h_1/h_3 = 1/3$. The curves 1,2 and 3 are referred to the structures 1, 2 and 3

respectively of fig. 2.
From the analysis of such diagram it can be noted that the behaviour of the three model considered is similar and, as the h_1/a ratio decreases, there occurs an increase in the values of the moments and displacements and an increase in the difference of the three models behaviour.

4.2.2.) In order to complete the comparison between structures 1 and 2, the axial moment course has been determined in the different sections of the connection shell.
In figs. 15, 16, 17, 18 there is a comparison of the moment courses in the two cylindrical connection shells computed for different values of l_2, for $h_1/a = 1/35$ and for $h_1/h_3 = 1/3$. Curve 1 is referred to the cylindrical shell with a wall of constant thickness, curve 2 is referred to the cylindrical shell with a wall of linearly variable thickness. From the analysis of these curves it can be drawn that up to the maximum value of $l_2 \simeq 100$ mm. (Figs. 15 and 16), the moment course for the two considered moments is coincident with a good approximation. For higher values of l_2 it can be noted a gradual departure of the two curves; the curve relative to the moment in the cylindrical shell of constant section presents a higher value in the lower and a lower value in the upper end with respect to the curve relative to the moment in the cylindrical shell of variable section.
With the considered geometry, for values of l_2 of about 400 mm. (fig. 17) the moment value drawn from the upper end in the case of cylindrical shell with constant thickness is about 50% less than that computed when considering the cylindrical shell with variable thickness. For values of l_2 higher than 400 mm. (Fig. 18) the moment course in case of constant thickness presents more considerable oscillations, reaching the maximum value not in the structure outline but intermediate areas.

REFERENCES

|1| Reissner, E.,"On the theory of thin elastic shells", Reissner Anniversary Volume: Contributions to applied Mechanics - Ed. J.W. Edwards (1949).

|2| Zudans, Z., Tsi Chu Yen, Steigelmann, W.H., "Thermal stress techniques in the nuclear industry" - Ed. American Elsevier (1965).

|3| Biezeno, C.B., and Grammel, R., "Engineering Dynamics" - Blackie & Son, Ltd. London & Grasgow (1955).

SIMBOLS

$(n_\phi)_{i,j}$	Axial normal load
$(n_\theta)_{i,j}$	circunferential normal load
$(m_\phi)_{i,j}$	axial bending moment
$(m_\theta)_{i,j}$	circumferential bending moment
$H_{i,j}$	radial load
$X_{i,j}$	rotation
$u_{i,j}$	radial displacement
$(\sigma_\phi)_{i,j}$	axial normal stress
$(\sigma_\phi)_{i,j}$	circumferential normal stress
$N_{i,j}$	axial load
R,W,H,Q	external load
s, x	general coordinate
p	internal pressure
a_i	radius
h_i	thickness
l_i	axial length

index

i	general shell
j	general section

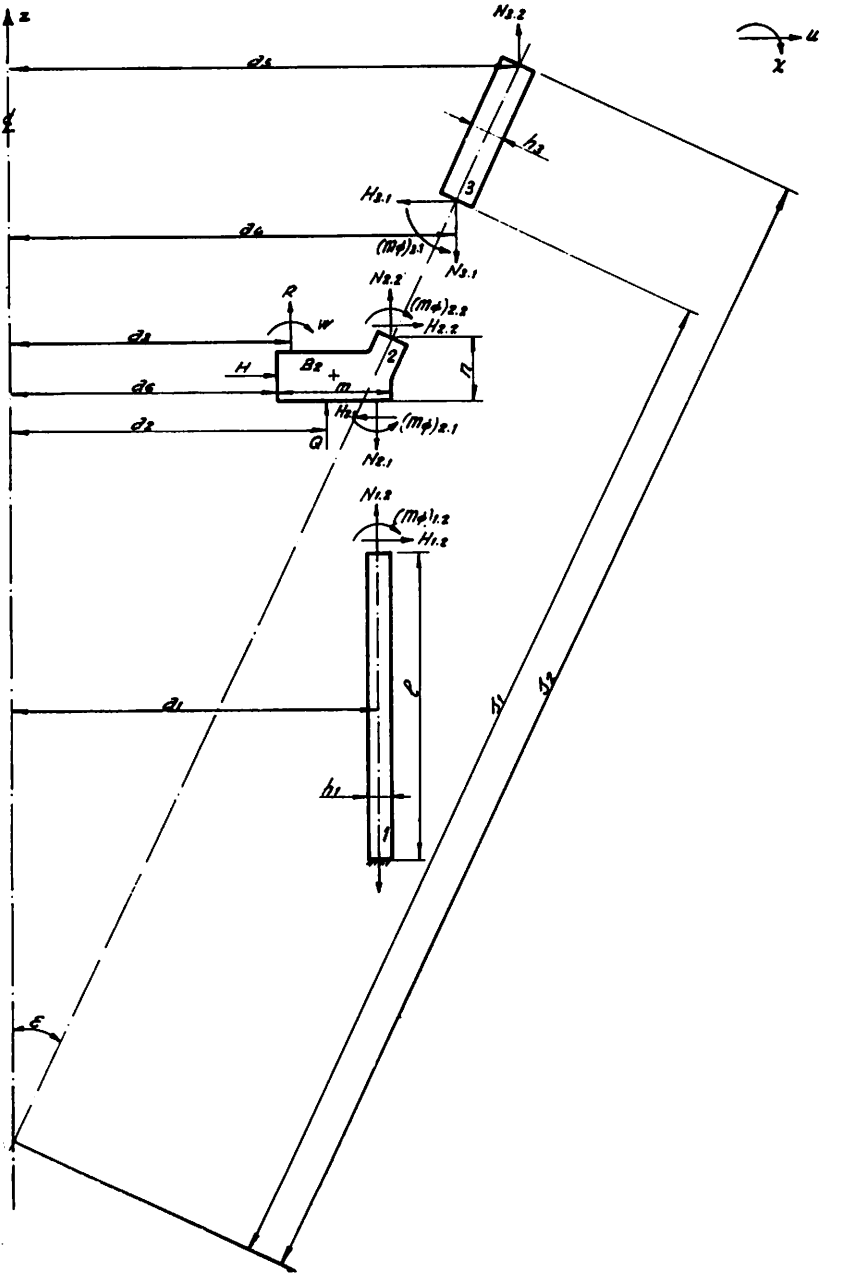

Fig. 1 - Support flange

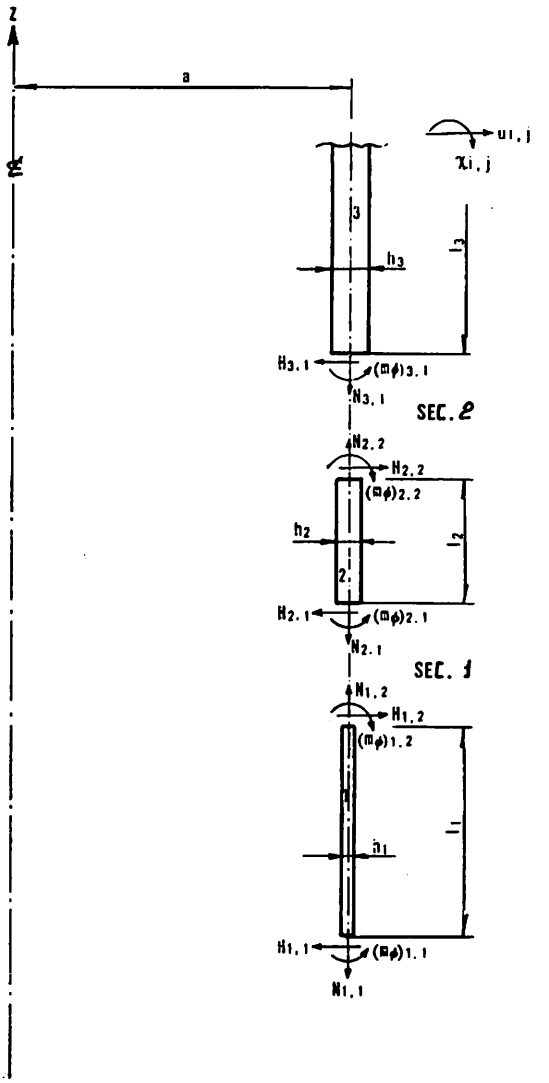

Fig. 2-1 - Cylindrical shell with wall of costant thickness- Structure 1

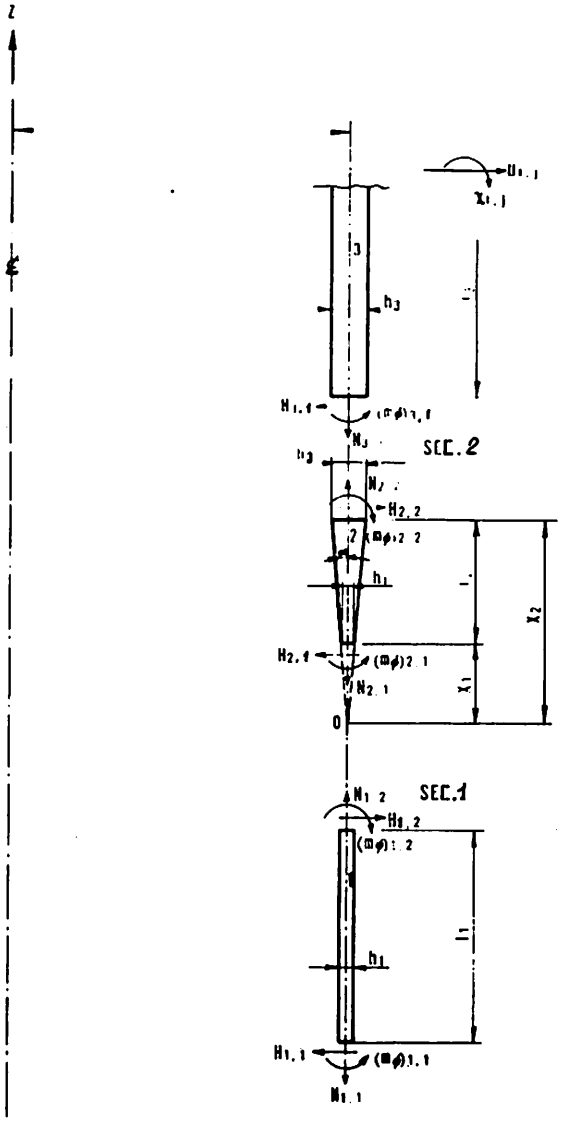

Fig. 2-2 - Cylindrical shell with wall of variable thickness- Structure 2

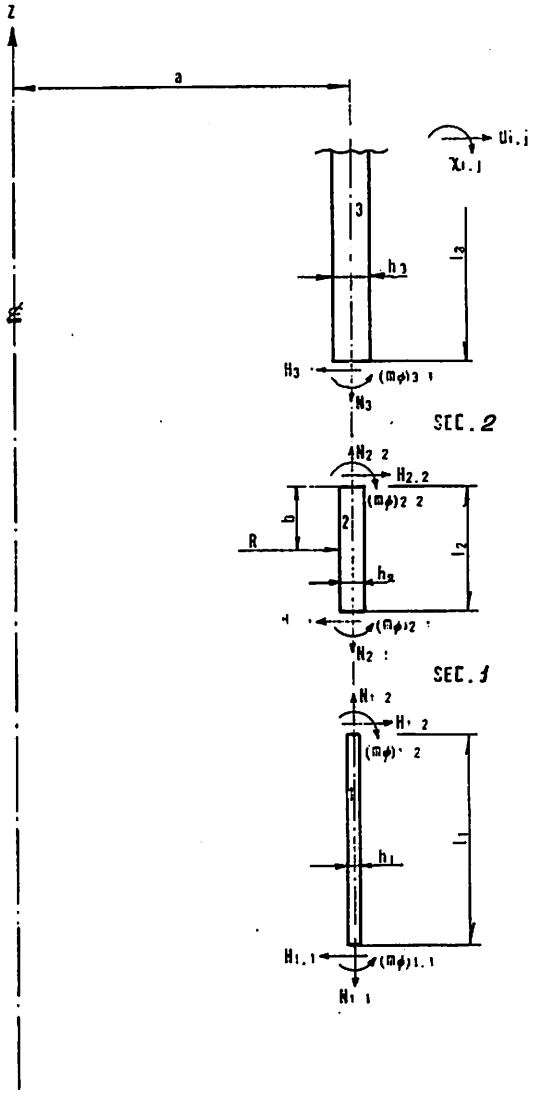

Fig. 2-3 - Axialsymmetrical rings - Structure 3

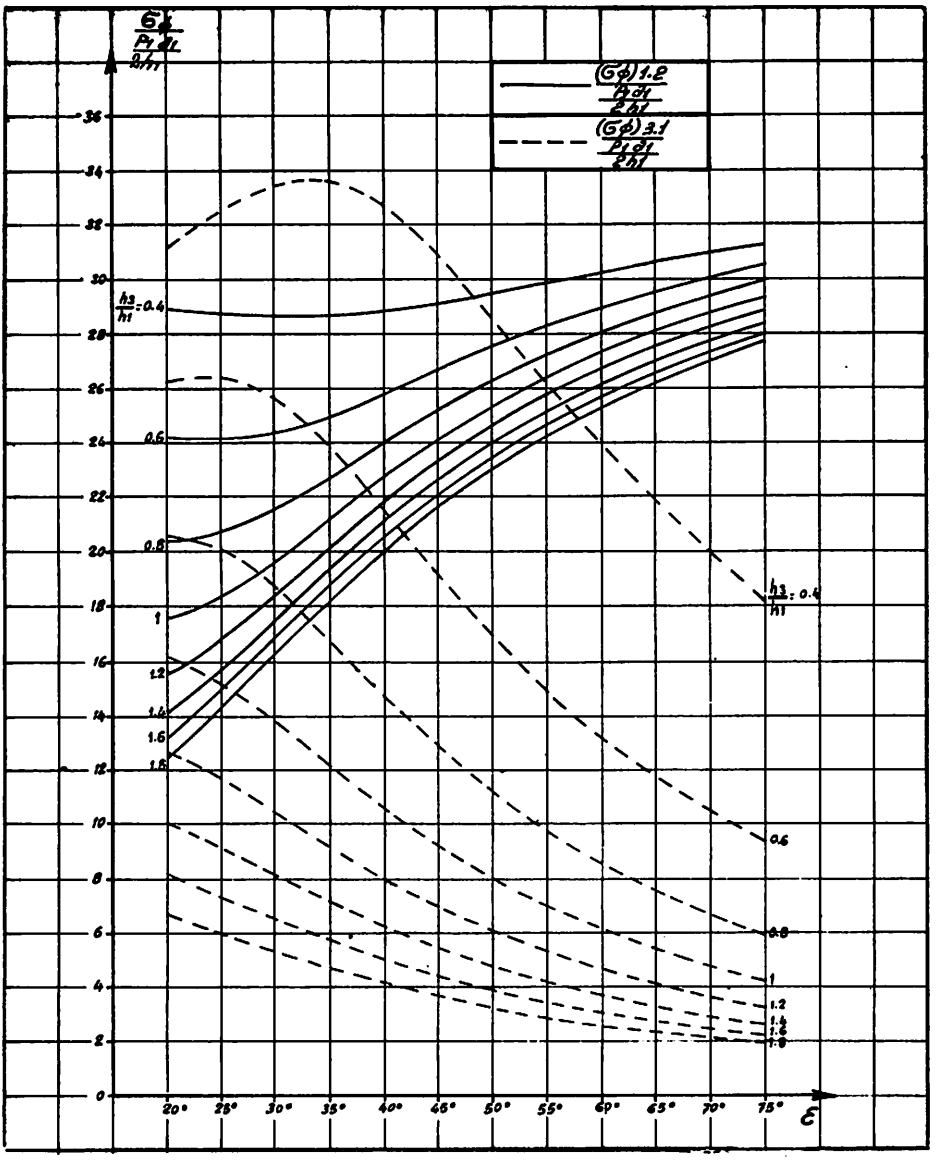

Fig. 3 - Axial normal stress (h_1 = 50 mm)

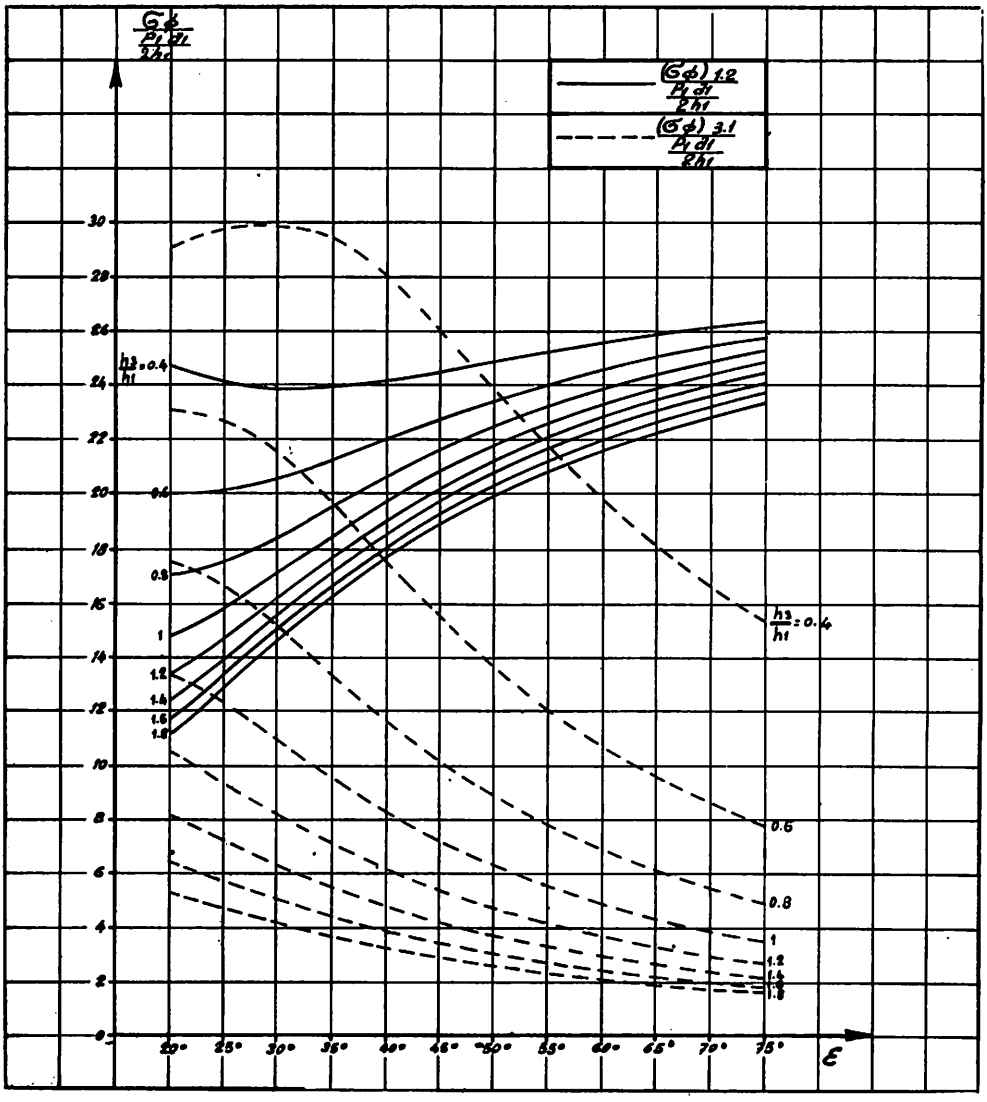

Fig. 4 - Axial normal stress (h_1 = 60 mm)

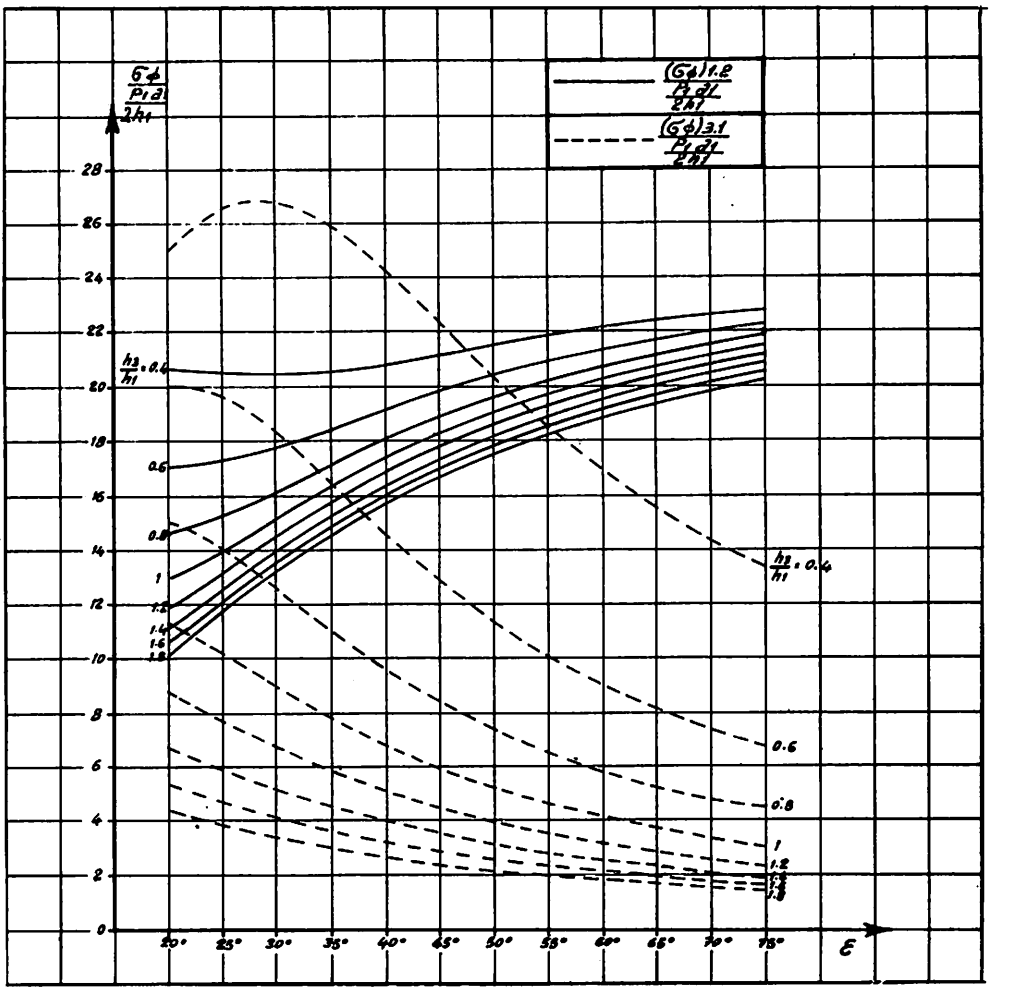

Fig. 5 - Axial normal stress (h_1 = 70 mm)

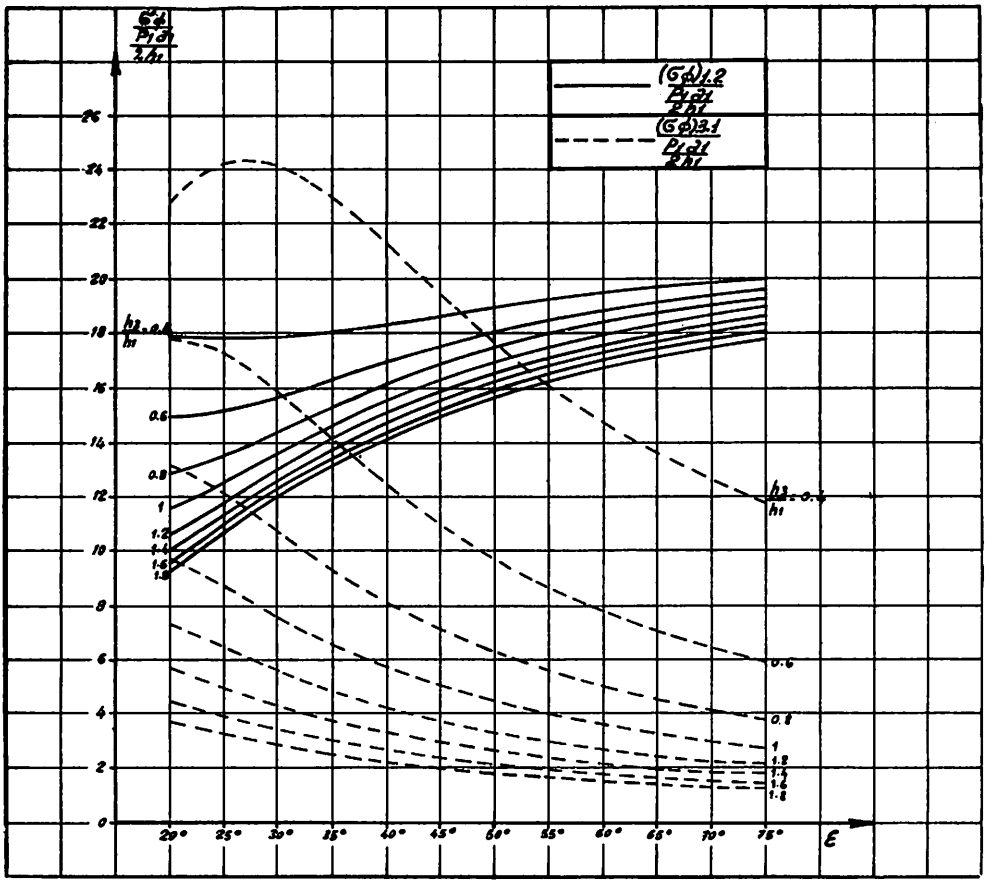

Fig. 6 - Axial normal stress (h_1 = 80 mm)

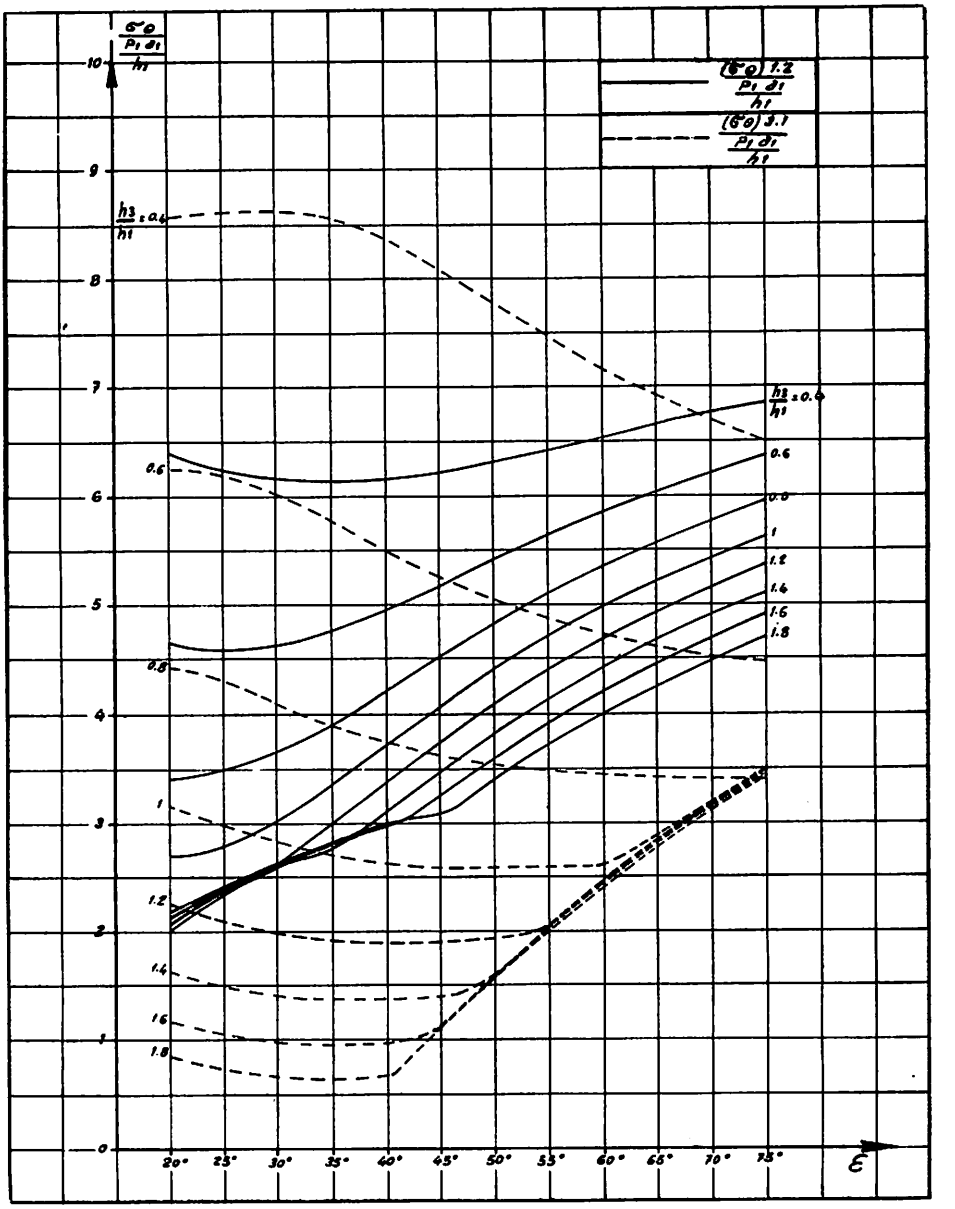

Fig. 7 - Circumferential normal stress (h_1 = 50 mm)

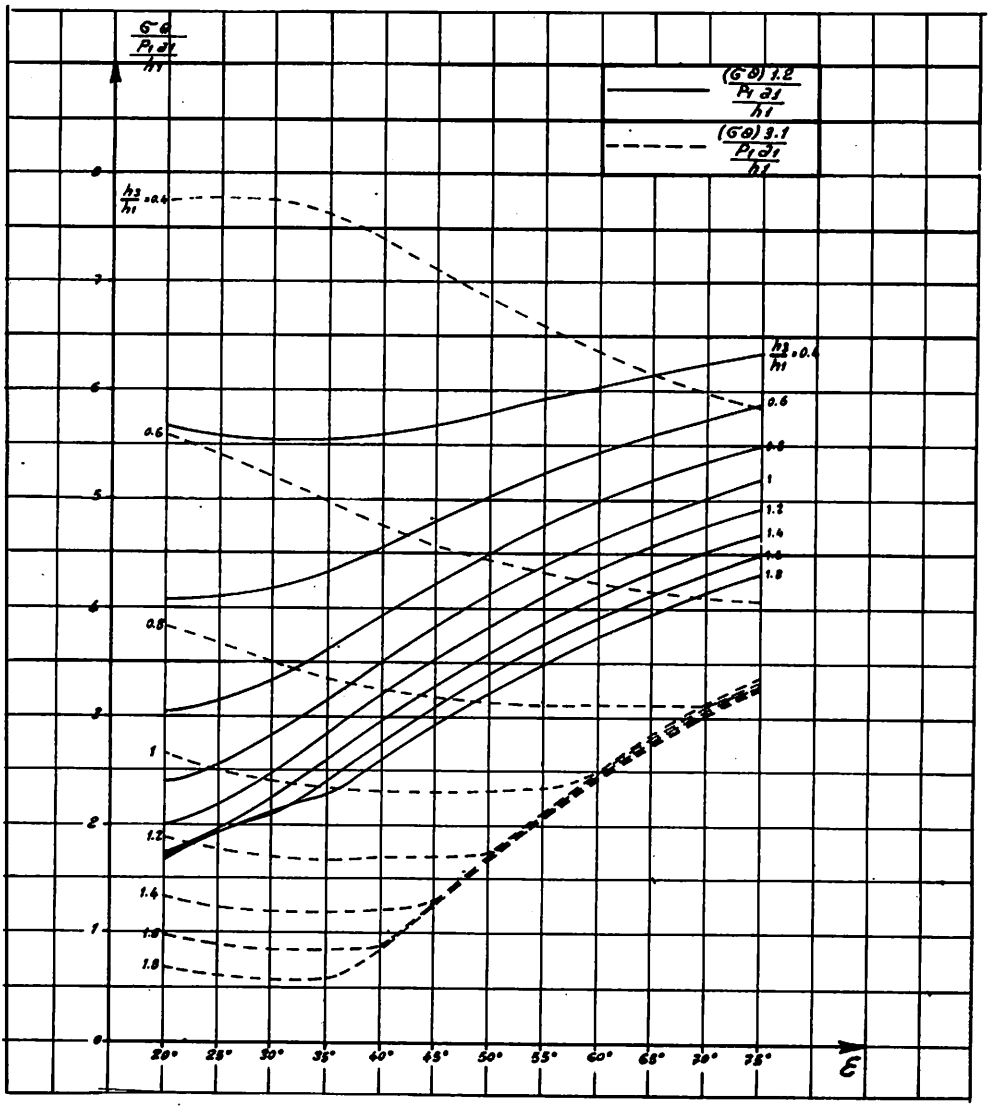

Fig. 8 - Circumfcrential normal stress (h_1 = 60 mm)

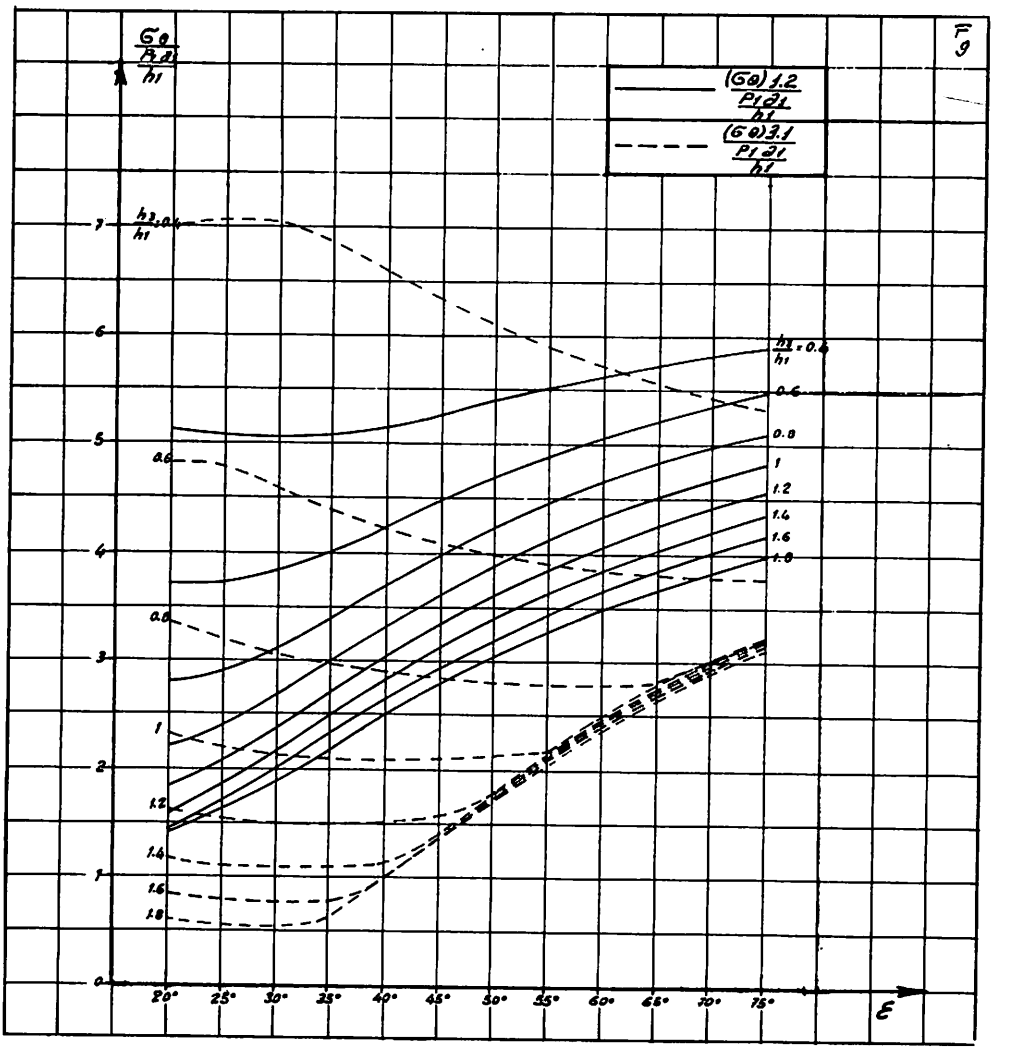

Fig. 9 - Circumferential normal stress (h_1 = 70 mm)

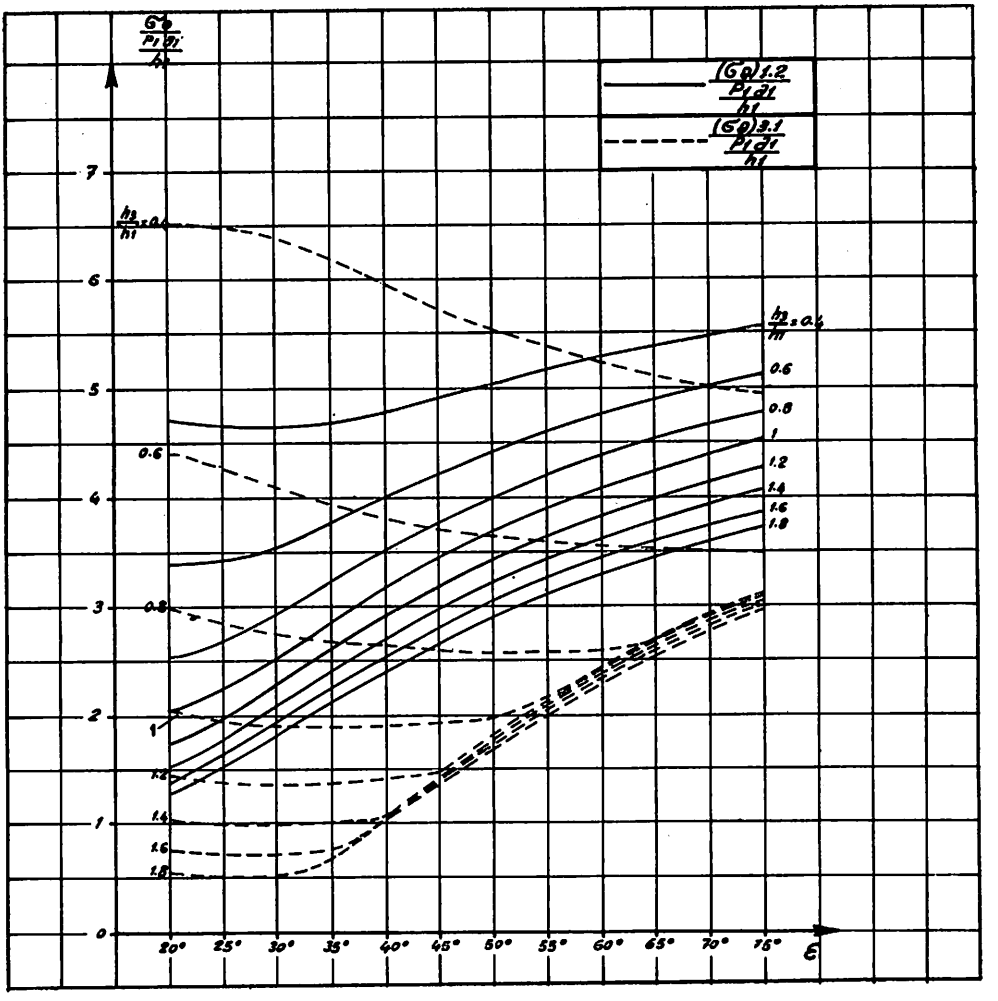

Fig. 10 - Circumferential normal stress (h_1 = 80 mm)

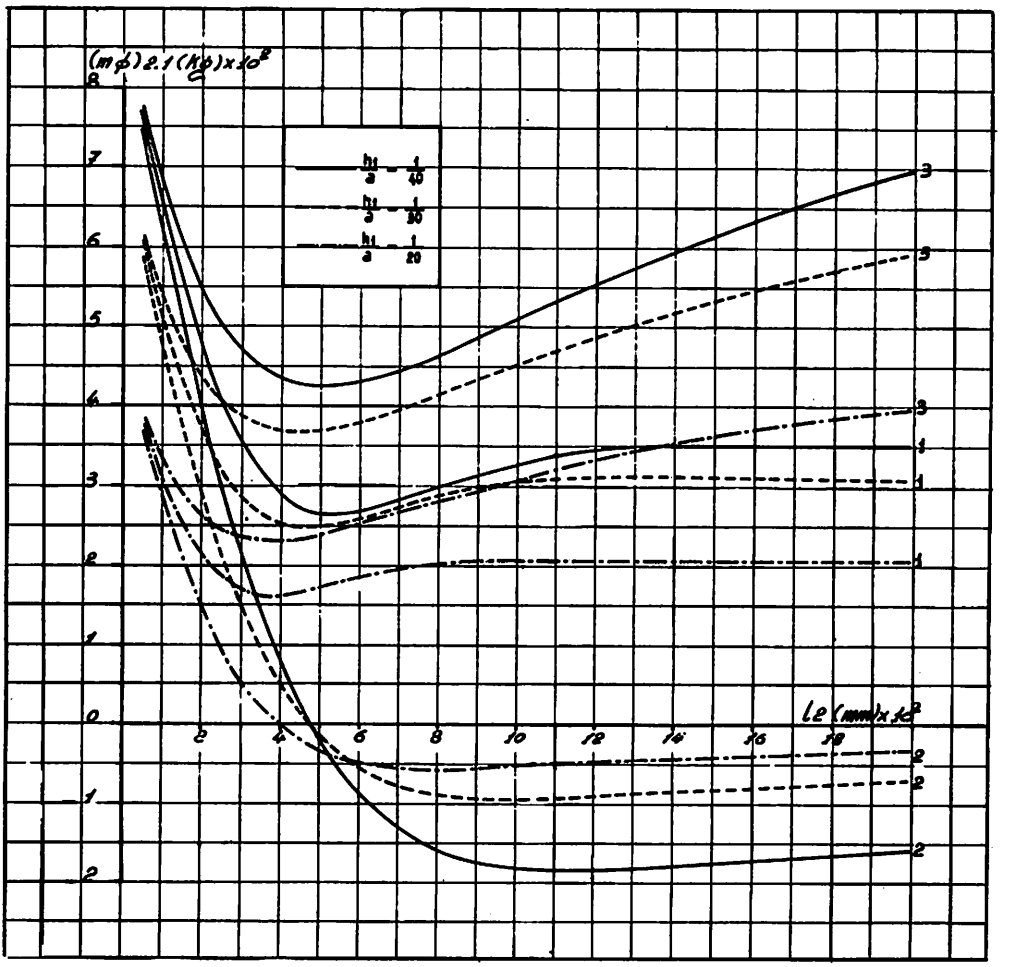

Fig. 11 - Axial bending moment in Sec. 1

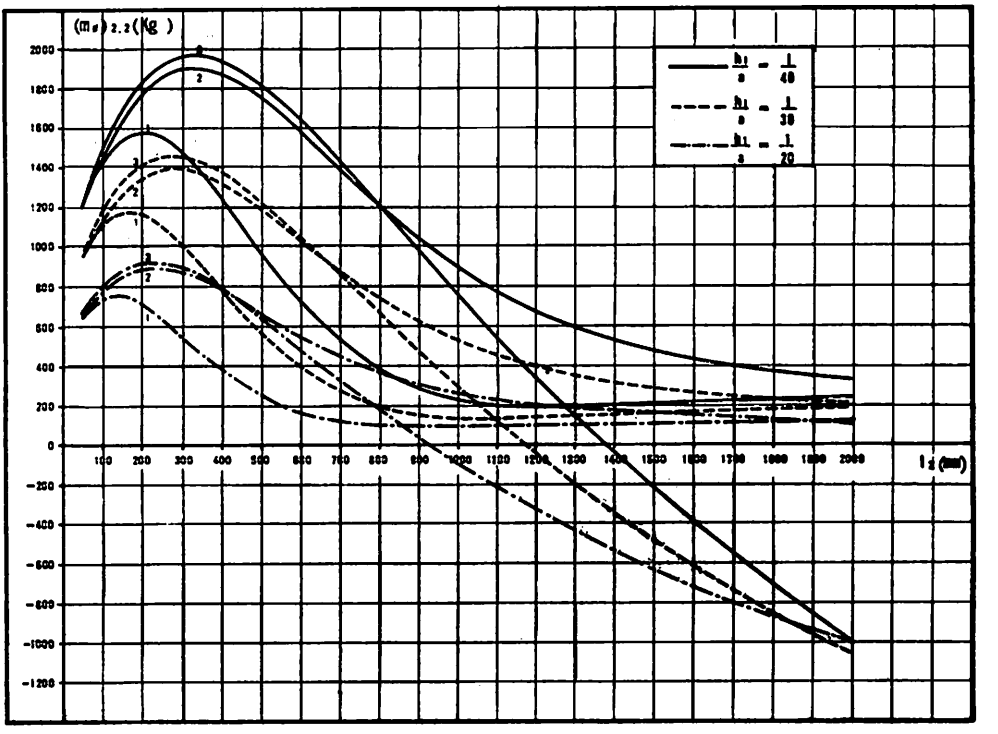

Fig. 12 - Axial bending moment in Sec. 2

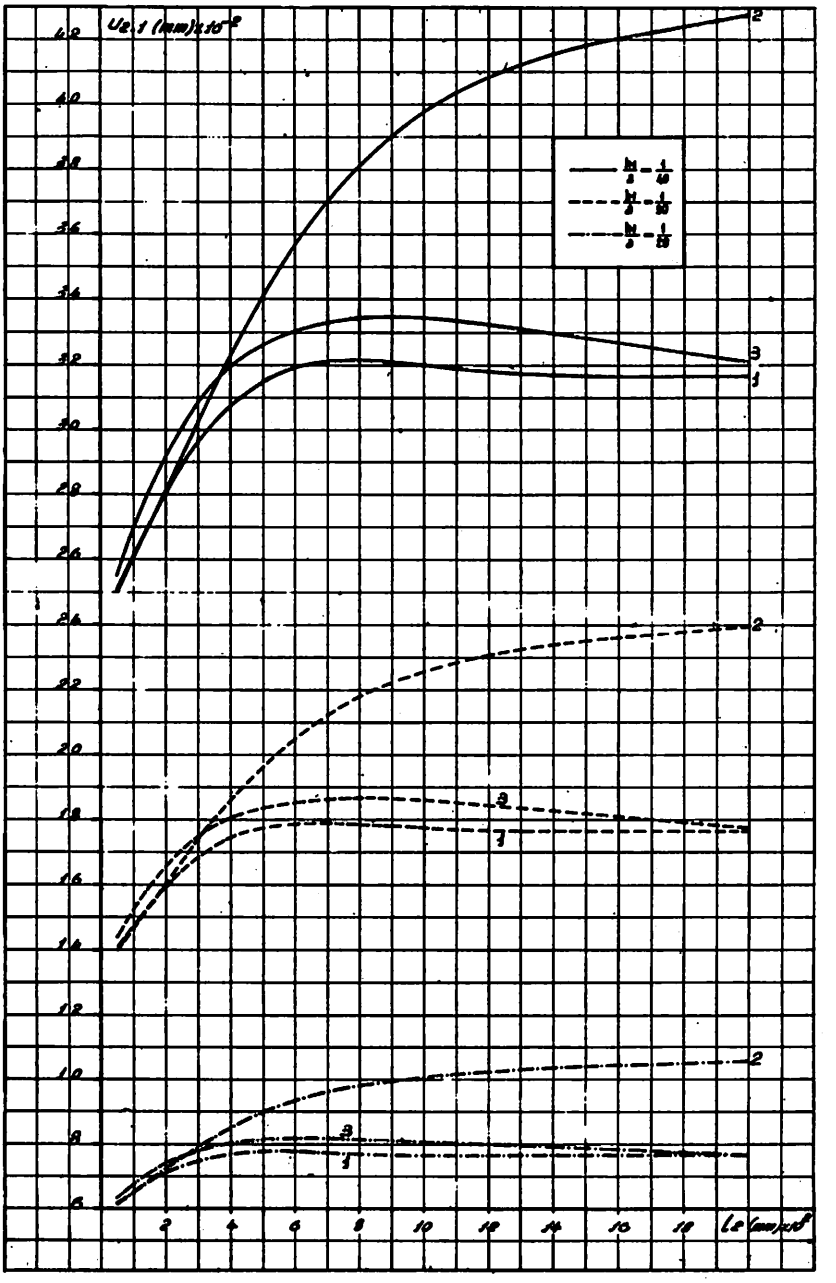

Fig. 13 - Radial displacement in Sec. 1

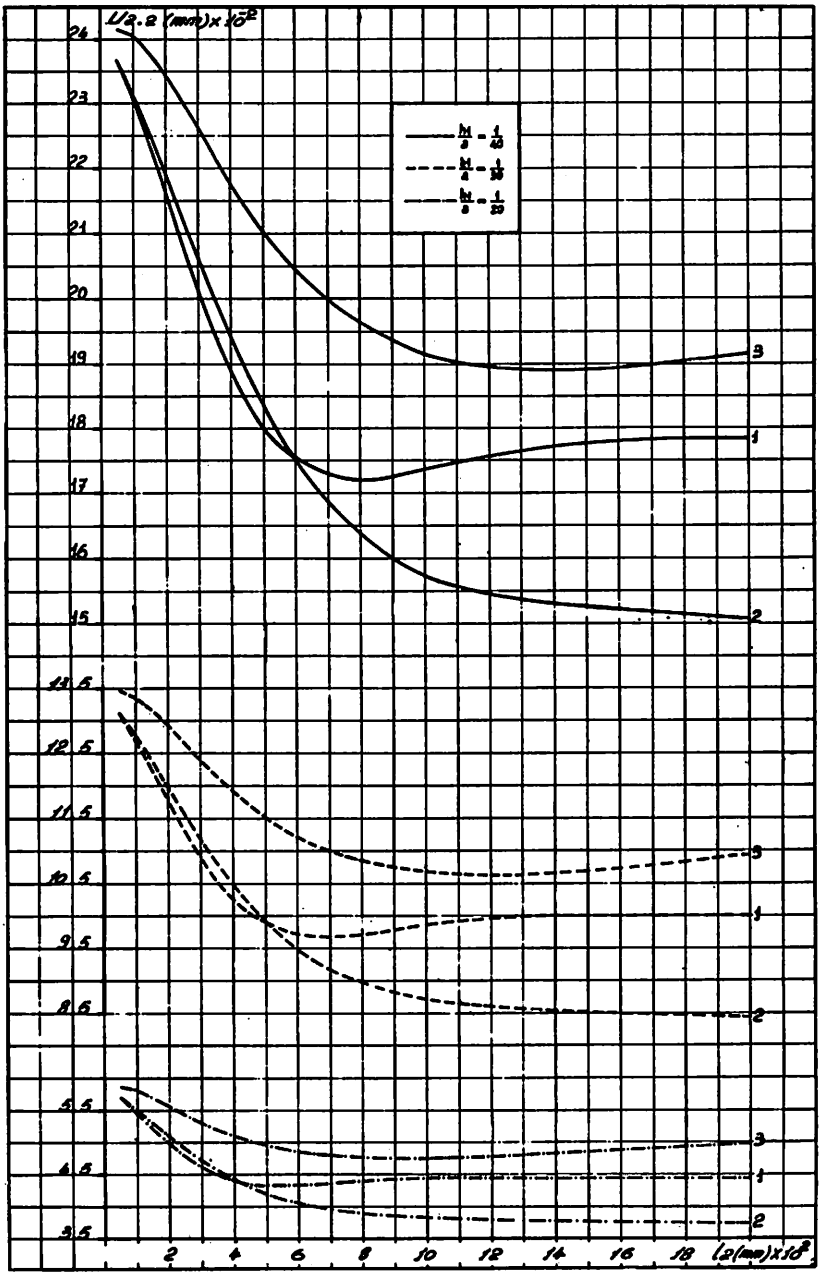

Fig. 14 - Radial displacement in Sec. 2

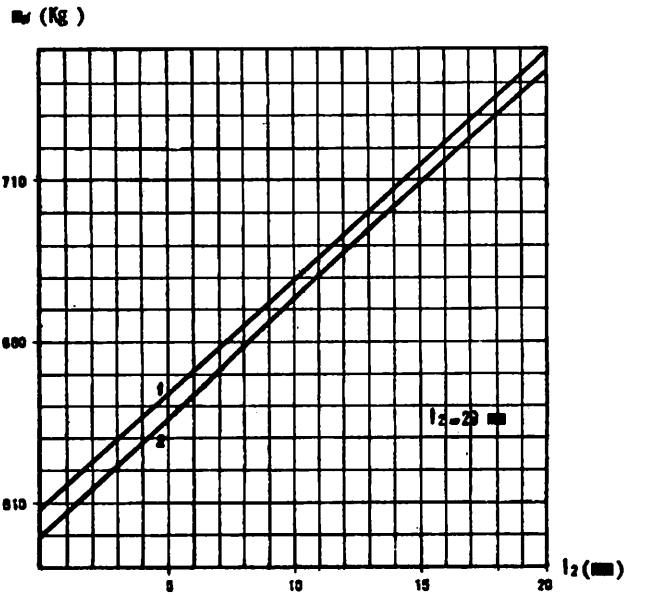

Fig. 15 - Axial bending moment (l_2 = 20 mm)

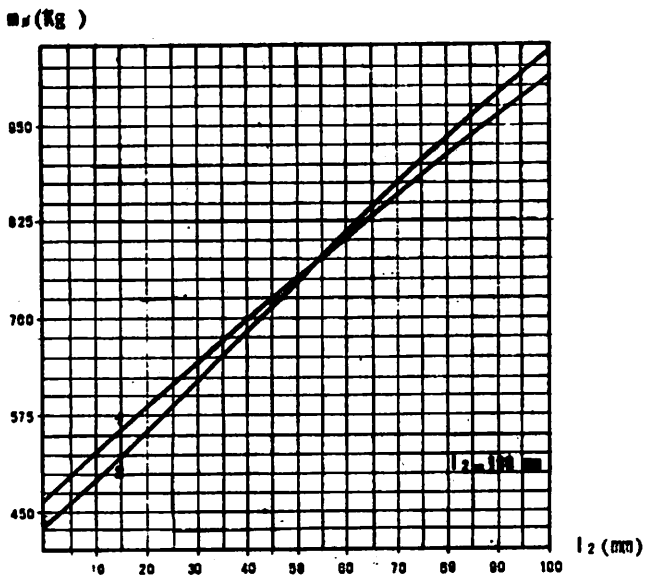

Fig. 16 - Axial bending moment (l_2 = 100 mm)

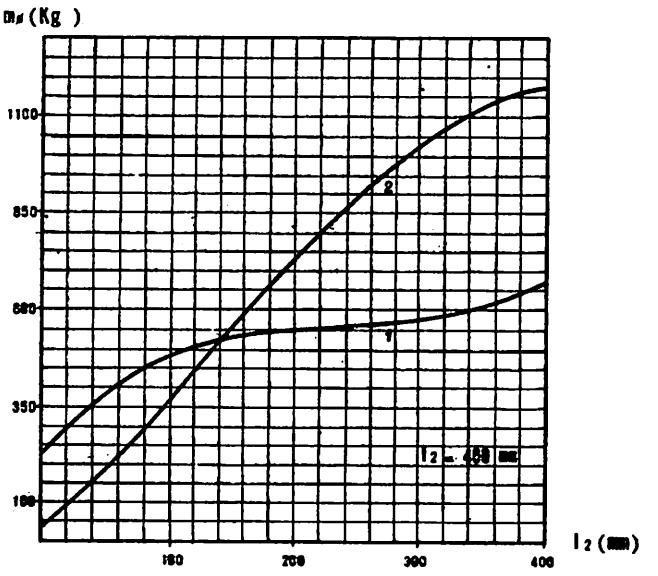

Fig. 17 - Axial bending moment (l_2 = 400 mm)

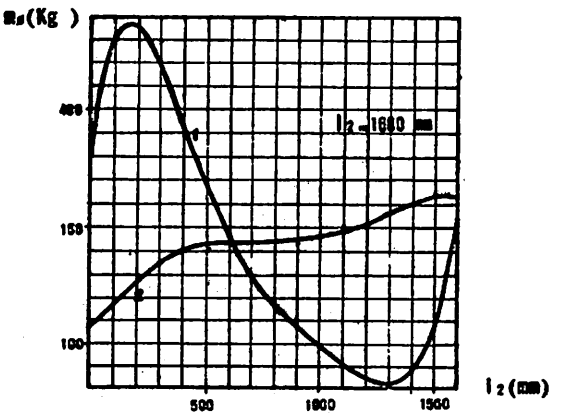

Fig. 18 - Axial bending moment (l_2 = 1600 mm)

DISCUSSION

Q W. O. LIVSEY, U. K.

Were thermal stresses included in the optimisation or were these not considered relevant in the optimisation ?

A S. CURIONI, Italy

The thermal stresses are not considered because in this case they are not relevant in this part of the vessel; it is possible in any case to take into account also this effect.